TNFα-stimulated gene-6 (TSG6) activates macrophage phenotype transition to prevent inflammatory lung injury

Manish Mittal[a], Chinnaswamy Tiruppathi[a], Saroj Nepal[a], You-Yang Zhao[a], Dagmara Grzych[a], Dheeraj Soni[a], Darwin J. Prockop[b,1], and Asrar B. Malik[a,1]

[a]Department of Pharmacology and Center for Lung and Vascular Biology, University of Illinois College of Medicine, Chicago, IL 60612 and [b]Institute for Regenerative Medicine, Texas A&M University Health Science Center and College of Medicine, Bryan, TX 77807

Contributed by Darwin J. Prockop, November 3, 2016 (sent for review September 7, 2016; reviewed by Arshad Rehman and Sarah Yuan)

TNFα-stimulated gene-6 (TSG6), a 30-kDa protein generated by activated macrophages, modulates inflammation; however, its mechanism of action and role in the activation of macrophages are not fully understood. Here we observed markedly augmented LPS-induced inflammatory lung injury and mortality in *TSG6*$^{-/-}$ mice compared with WT (*TSG6*$^{+/+}$) mice. Treatment of mice with intratracheal instillation of TSG6 prevented LPS-induced lung injury and neutrophil sequestration, and increased survival in mice. We found that TSG6 inhibited the association of TLR4 with MyD88, thereby suppressing NF-κB activation. TSG6 also prevented the expression of proinflammatory proteins (iNOS, IL-6, TNFα, IL-1β, and CXCL1) while increasing the expression of anti-inflammatory proteins (CD206, Chi3l3, IL-4, and IL-10) in macrophages. This shift was associated with suppressed activation of proinflammatory transcription factors STAT1 and STAT3. In addition, we observed that LPS itself up-regulated the expression of TSG6 in *TSG6*$^{+/+}$ mice, suggesting an autocrine role for TSG6 in transitioning macrophages. Thus, TSG6 functions by converting macrophages from a proinflammatory to an anti-inflammatory phenotype secondary to suppression of TLR4/NF-κB signaling and STAT1 and STAT3 activation.

medical sciences | biological sciences | immunology | inflammation | acute lung injury

TNFα-stimulated gene-6 (TSG6) is a 30-kDa hyaluronan (HA)-binding protein produced by monocytes/macrophages, mesenchymal stem cells (MSCs), and fibroblasts in inflammatory diseases (1–4). However, there appears to be little constitutive expression of TSG6 (3). TSG6 is synthesized in response to proinflammatory mediators, including lipopolysaccharide (LPS), TNFα, and IL-1β (3–5). TSG6 is composed of an HA-binding LINK domain and a CUB (complement protein subcomponents C1r/C1s, urchin embryonic growth factor, and bone morphogenetic protein) domain (3, 4) To date, only the HA-binding protein CD44 has been shown to function as a TSG6 receptor (6).

TSG6 has a potent but poorly understood function in suppressing inflammation through inhibition of neutrophil migration and production of proinflammatory cytokines (7, 8). This effect of TSG6 has been demonstrated in several models. TSG6 was shown to prevent inflammation and tissue injury in rodent models of arthritis (9), myocardial infarction (10), corneal injury (11), and peritonitis (12). Both IL-1β and TNFα induced the synthesis of TSG6 in MSCs, monocytes/macrophages, and fibroblasts (2, 4, 5). Administration of human MSCs in mice prevented endotoxin (LPS)-induced acute lung injury (ALI), and, importantly, this effect was abrogated using cells pretreated with TSG6-siRNA to suppress TSG6 expression (13). TSG6 also delayed the onset of autoimmune diabetes by suppressing the activation of T cells and antigen-presenting cells (14), further supporting its role in dampening the adaptive immune response.

In the present study, we addressed the role of TSG6 in ALI, an acute inflammatory disease that injures the lung's vascular barrier, resulting in severe protein-rich pulmonary edema and hypoxemia, associated with ~50% mortality (15). There is a profound release of proinflammatory cytotoxic mediators from activated alveolar macrophages and other inflammatory cells sequestered in lungs (15). Macrophages in ALI are activated through the sensing of pathogen-associated molecular patterns (PAMPs) and damage-associated molecular patterns (DAMPs) via Toll-like receptors (TLRs). On binding of LPS to TLR4, macrophages produce proinflammatory cytokines, such as IFNγ, TNFα, and IL-1β, which signal the recruitment of neutrophils and lymphocytes at the site of infection and aid in the clearance of pathogens (16). However, macrophages also display marked plasticity and functional heterogeneity depending on such factors as their niche, interaction with other cells (e.g., endothelial cells), and cytokines to which they are exposed (17, 18).

Macrophages are classified as classically activated macrophages, or M1 type, and alternatively activated macrophages, or M2 type (17, 18). Within this classification, macrophages are polarized to the M1 in response to LPS and other mediators, such as IFNγ, whereas M2 macrophages are generated in response to IL-4, IL-10, and glucocorticoids (18–20). Each type is characterized by distinct molecular signatures, such as iNOS, IL-12, IL-6, TNFα, and STAT1 for M1 and arginase-1, chitinase-3-like-3 (Chi3l3), IL-10, IL-4, and STAT6 for M2 (17–20). However, recent transcription data indicate that macrophages exhibit a far more complex range of phenotypes than are accounted for by the M1/M2 classification scheme (17–20). The basis for macrophage polarization in vivo is not clear, but NF-κB activation downstream of TLR4 and up-regulation of specific cytokines and transcription factors, such as STAT6, appear to be important in mediating macrophage plasticity (20–24).

We examined the role of TSG6, a macrophage releasate, in mediating the phenotypic shift of macrophages and in counteracting LPS-induced ALI in mice. We found that TSG6 is crucial in mediating the transition of macrophages and thereby inhibiting the inflammatory feed-forward cascade activated by LPS. We show that the TSG6-mediated reprogramming of macrophages is essential

Significance

We found that TNFα-stimulated gene-6 (TSG6), a secreted 30-kDa immunomodulatory protein, resolved LPS-induced inflammatory lung injury by shifting macrophages from a proinflammatory to an anti-inflammatory phenotype. Macrophages from mice genetically deficient in TSG6 failed to transition, demonstrating the essential role of TSG6 in mediating macrophage plasticity. The finding that TSG6 induced the marked transition in anti-inflammatory macrophages lays the foundation for its therapeutic application.

Author contributions: M.M., Y.-Y.Z., D.J.P., and A.B.M. designed research; S.N., D.G., and D.S. performed research; M.M., S.N., D.G., D.S., and D.J.P. analyzed data; and M.M., C.T., D.J.P., and A.B.M. wrote the paper.

Reviewers: A.R., University of Rochester Medical Center; and S.Y., University of South Florida.

Conflict of interest statement: D.J.P. is chair of the Scientific Advisory Committee and has a small equity stake (<5%) in Temple Therapeutics, LLC, with an interest in TSG6.

[1]To whom correspondence may be addressed. Email: abmalik@uic.edu or Prockop@medicine.tamhsc.edu.

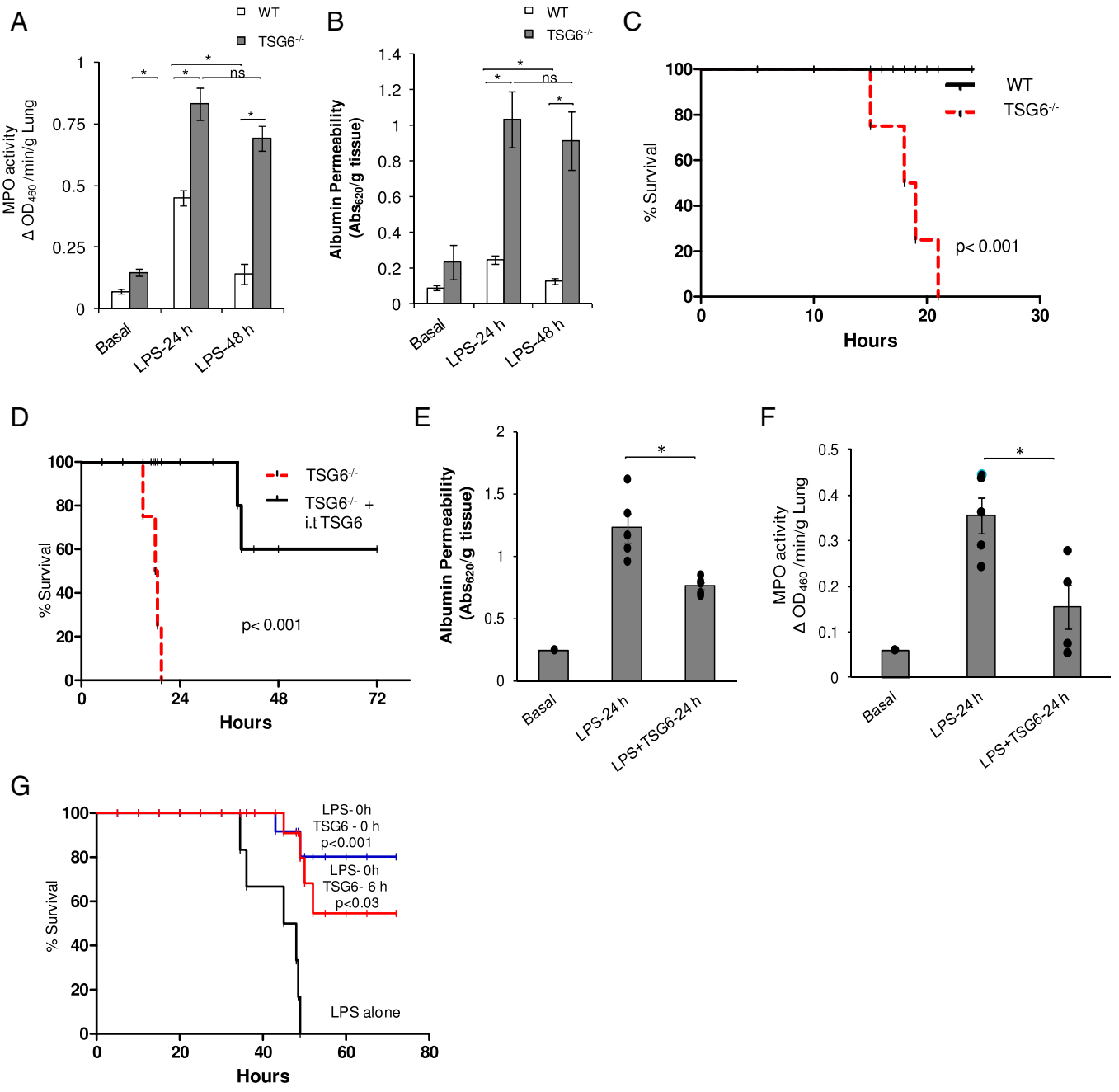

Fig. 1. TSG6 deletion in mice ($TSG6^{-/-}$) augments LPS-induced inflammatory lung injury. (*A* and *B*) WT ($TSG6^{+/+}$) and $TSG6^{-/-}$ mice were challenged with LPS (10 mg/kg i.p.). (*A*) Lungs obtained at 0, 24 h, and 48 h after LPS challenge were used to measure MPO activity in lungs. (*B*) After LPS challenge, lung vascular permeability (uptake of EBA) was assessed. $n = 4$ mice per time point. $^*P < 0.05$, WT vs. $TSG6^{-/-}$. (*C*) Survival of age- and weight-matched WT and $TSG6^{-/-}$ mice monitored after challenge with a lethal dose of LPS (20 mg/kg i.p.). $TSG6^{-/-}$ mice showed the highest mortality within 20 h after LPS injection compared with WT mice. $n = 10$ per group. $^*P < 0.001$, WT vs. $TSG6^{-/-}$. (*D*) Survival of $TSG6^{-/-}$ mice challenged with LPS (20 mg/kg, i.p.) with and without simultaneous i.t. instillation of TSG6 (5 μg/mouse). TSG6 instillation rescued the high mortality seen in the $TSG6^{-/-}$ mice, increasing survival by 60% compared with untreated controls. $n = 8$ mice per group. $^*P < 0.001$. (*E* and *F*) WT mice were simultaneously challenged with LPS (10 mg/kg, i.p.) and saline (i.t) or TSG6 (5 μg/mouse, i.t.). (*E*) At 0 and 24 h after LPS/saline or LPS/TSG6 administration, mice were used for lung EBA permeability measurements as above. Mice treated with TSG6 showed significantly reduced lung vascular permeability compared with untreated control mice. $n = 5$ mice per group; $^*P < 0.05$, LPS vs. LPS + TSG6. (*F*) At 0 and 24 h after LPS/saline or LPS/TSG6 administration, lungs were used to measure MPO activity, expressed as change in absorbance (ΔA). MPO activity was significantly reduced in lungs of TSG6-treated mice compared with saline-treated control mice. $n = 4$ mice per group. $^*P < 0.05$, LPS vs. LPS + TSG6. (*G*) Survival in WT mice, monitored for 72 h after a lethal dose of LPS (20 mg/kg i.p.) alone or in combination with TSG6 (5 μg/mouse) given i.t. either concomitantly with or 6 h after LPS challenge. $n = 10$ per group. $^*P < 0.001$, LPS vs. LPS + TSG6; $^*P < 0.03$, LPS vs. LPS + TSG6 post-LPS.

for the resolution of ALI. The expression of anti-inflammatory macrophage signatures (arginase-1 and Chi3l3) was abrogated in $TSG6^{-/-}$ mice, whereas the expression of proinflammatory transcription factors STAT1 and STAT3 was enhanced. TSG6 expression in macrophages was itself increased in response to LPS, resulting in a cell population displaying a distinct anti-inflammatory

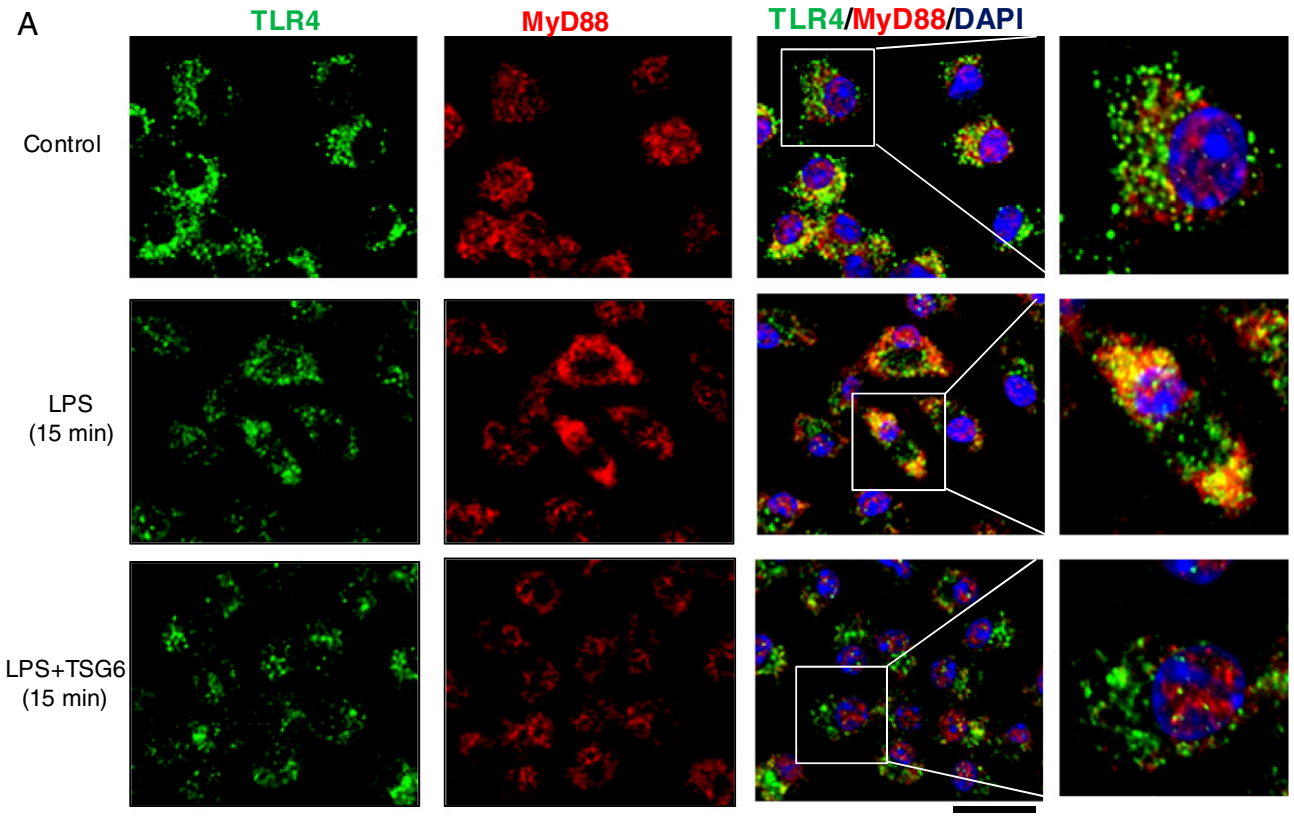

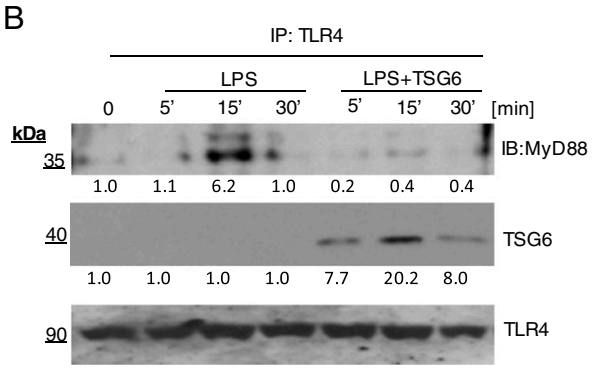

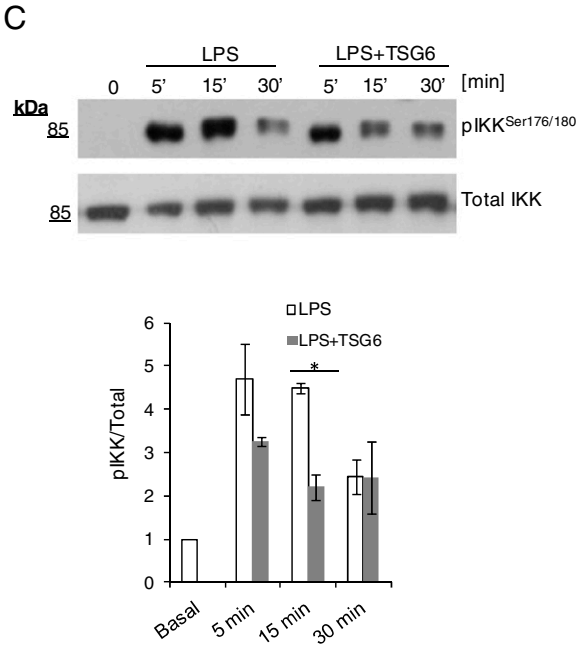

Fig. 2. TSG6 inhibits the interaction of TLR4 with MyD88 and prevents NF-κB activation. (*A*) Macrophages cultured from bone marrow of WT mice were challenged with LPS (1 μg/mL) alone or TSG6 (0.1 μg/mL) plus LPS (1 μg/mL) together for 0 and 15 min. Cells were fixed, permeabilized, and stained, and images were acquired by confocal microscopy. Green, TLR4; red, MyD88; blue, DAPI. Strong colocalization of TLR4 with MyD88 was seen after LPS challenge, and this response was prevented by rTSG6. (Scale bar: 20 μm.) (*B*) WT macrophages cultured from bone marrow were treated with LPS (1 μg/mL) alone or with rTSG6 (0.1 μg/mL) plus LPS (1 μg/mL) for different times. They were then lysed and immunoprecipitated with anti-TLR4 polyclonal antibody (pAb). Immunoprecipitated samples were blotted with anti-MyD88 or anti-TSG6 pAb, and blots were reprobed with anti-TLR4 pAb. A strong interaction of MyD88 with TLR4 was observed at 15 min after LPS treatment, which was abolished by rTSG6. (*C*) The cell lysates were immunoblotted with anti–phos-Ser177/181-IKKβ pAb. Quantified results are shown as ratio of phosphorylated to total protein (*Bottom*). rTSG6 treatment decreased LPS-induced phosphorylation of IKKβ. **P* < 0.05, LPS vs. LPS + TSG6.

phenotype. This indicates that TSG6 plays a vital role in the resolution of inflammatory lung injury in vivo by converting macrophages to the anti-inflammatory phenotype, and furthermore, that TSG6 expression is a strong indicator of the innate immune function of macrophages.

Results

TSG6 Deletion (*TSG6*$^{-/-}$) in Mice Augments Lung Vascular Injury, Neutrophil Sequestration, and Mortality Induced by LPS. We challenged *TSG6*$^{-/-}$ mice with 20 mg/kg LPS i.p. and measured lung vascular permeability (an index of vascular injury) using Evans blue dye conjugated with albumin (EBA) tracer and neutrophil sequestration by assaying lung tissue myeloperoxidase (MPO) content. *TSG6*$^{-/-}$ mice showed a higher basal MPO level compared with WT mice, although the basal vascular permeability value was not significantly greater than that in WT mice (Fig. 1 *A* and *B*). However, at 24 h after LPS challenge, *TSG6*$^{-/-}$ mice demonstrated significantly greater lung vascular injury and neutrophil accumulation compared with WT mice (Fig. 1 *A* and *B*). In contrast, at 48 h after LPS challenge, lung vascular injury and neutrophil sequestration both recovered to basal values in WT mice, but persisted in *TSG6*$^{-/-}$ mice (Fig. 1 *A* and *B*). We also observed 100% mortality in *TSG6*$^{-/-}$ mice (generated on a BALB/c background) within 20 h of the LPS challenge, whereas all WT mice of the same background survived (Fig. 1*C*), consistent with the survival results reported in other studies in mice of the BALB/c strain given LPS (25).

Next, to determine whether exogenous administration of TSG6 was itself protective, we evaluated the effects of intratracheal (i.t.) instillation of recombinant (r) TSG6. We observed that *TSG6*$^{-/-}$ mice treated with rTSG6 before LPS challenge showed 60% survival, compared with no survival of *TSG6*$^{-/-}$ mice (Fig. 1*D*). Thus, TSG6 administration significantly reduced the mortality seen in *TSG6*$^{-/-}$ mice.

TSG6 Treatment Prevents LPS-Induced Lung Vascular Injury, Neutrophil Infiltration, and Mortality. We challenged WT mice with i.p. LPS and simultaneously instilled rTSG6 i.t., and then at 24 h post-LPS challenge assessed lung vascular injury and neutrophil uptake as above. rTSG6 significantly reduced LPS-induced lung vascular injury and neutrophil sequestration (Fig. 1 *E* and *F*). To investigate the prophylactic vs. therapeutic effects of rTSG6, we divided the mice into three groups. Group I was challenged with i.p. LPS alone, group 2 received concomitant i.p. LPS and i.t. rTSG6, and group 3 received i.t. rTSG6 at 6 h post-LPS challenge, when the mice had a high probability of dying. In group 1 (LPS alone), all mice died within 48 h of the LPS challenge (Fig. 1*G*). Group 2 (concomitant rTSG6 and LPS) showed 80% survival, and, surprisingly, group 3 mice (rTSG6 at 6 h post-LPS) showed 50% survival (Fig. 1*G*).

TSG6 Prevents the Interaction of TLR4 with MyD88 and NF-κB Activation. We next determined whether rTSG6 interfered with TLR4 signaling, which induces NF-κB activation via MyD88-dependent and MyD88-independent pathways (26). In control bone marrow-derived macrophages, LPS induced IκB kinase β (IKKβ) phosphorylation within 5 min; however, a strong TLR4–MyD88 association was observed only within 15 min (Fig. 2 *A*–*C*). rTSG6 suppressed IKKβ activation and inhibited the association of MyD88 with TLR4 (Fig. 2 *A*–*C*); thus, TSG6 functions by preventing MyD88-dependent NF-κB activation.

TSG6 Reprograms Macrophage Phenotype in Vivo. To investigate mechanisms of TSG6 inhibition of LPS-induced ALI, we injected mice with i.p. LPS (10 mg/kg) alone or concomitantly with i.t. rTSG6 (5 μg/mouse). At 6 h and 24 h after LPS, we measured concentrations of proinflammatory cytokines IL-6, TNFα, IFNγ, and IL-12p70 and anti-inflammatory cytokines IL-10 and IL-4 in bronchoalveolar lavage (BAL) fluid. TSG6 treatment significantly reduced the generation of IL-6, IFNγ, TNFα, and IL-12p70 while increasing the generation of IL-10 and IL-4 (Fig. 3 *A* and *B*). In other experiments, we obtained CD11b^{+} cells (alveolar macrophages) from BAL fluid of mice at 24 h post-LPS. TSG6 treatment of these mice suppressed the LPS-mediated induction of proinflammatory transcripts iNOS, IL-6, TNFα, IL-1β, and CXCL1 while augmenting anti-inflammatory markers CD206 and Chi3l3 in the alveolar macrophages (Fig. 3*C*).

We also isolated CD11b^{+} macrophages from digested lungs at 24 h after challenging mice with either i.p. LPS or i.p. LPS plus TSG6, and assessed the expression of proinflammatory and anti-inflammatory proteins by Western blot analysis and ELISA. rTSG6 suppressed the phosphorylation of the proinflammatory transcription factors STAT1 and STAT3, as well as the expression of IL-1β in these cells (Fig. 4*A*). Interestingly, the CD11b^{+} cells obtained from the rTSG6-treated mice showed increased expression of arginase-1 and Chi3l3, indicative of the anti-inflammatory phenotype shift (Fig. 4*A*).

We next placed the CD11b^{+} cells in culture for 3 d, and then used the culture supernatants for cytokine measurements. We observed that CD11b^{+} macrophages obtained from the mice treated with TSG6 exhibited reduced production of TNFα, IL-6, IFNγ, and IL-12p70 and increased production of IL-10 and IL-4 (Fig. 4*B*).

In these studies, we also determined whether LPS itself could could up-regulate TSG6 expression. We observed that LPS given i.p. induced the TSG6 expression in the lungs of WT mice, but not of *TSG6*$^{-/-}$mice (Fig. 4*C*). LPS also induced phosphorylation of the proinflammatory transcription factors STAT1 and STAT3 at 6 h of the LPS challenge in *TSG6*$^{+/+}$ mice, followed by a return to baseline at 24 h (Fig. 4*C*). In contrast, LPS induced sustained phosphorylation of STAT1 and STAT3 in *TSG6*$^{-/-}$ mice (Fig. 4*C*), indicating that TSG6 regulates STAT1 and STAT3 activities. Importantly, LPS induced a sustained expression of IL-1β in *TSG6*$^{-/-}$ mice, but not in *TSG6*$^{+/+}$ mice (Fig. 4*C*), suggesting the crucial role of TSG6 in dampening inflammation. We also observed that expression of anti-inflammatory proteins arginase-1 and Chi3l3 was increased in *TSG6*$^{+/+}$ mice post-LPS, whereas their expression was defective in *TSG6*$^{-/-}$ mice (Fig. 4*C*).

Discussion

TSG6 was first described as an anti-inflammatory factor released by TNFα-treated fibroblasts (27, 28). IL-1β and TNFα have been shown to induce TSG6 expression in multiple cell types (2–5, 29). Human and murine TSG6 proteins are ∼94% identical (4). Transgenic mice overexpressing TSG6 were resistant to collagen-induced arthritis (CIA) (9), whereas inactivation of the TSG6 gene enhanced inflammation and increased the susceptibility to arthritis (30). Intravenous administration of MSCs in mice also prevented endotoxin-mediated ALI, apparently by reducing the expression of proinflammatory cytokines and neutrophil sequestration in lungs (13); however, siRNA-mediated suppression of TSG6 expression in MSCs prevented these protective effects, indicating the involvement of TSG6 in this protection. In another study, TSG6 prevented zymosan-induced peritonitis secondary to reduced TLR2-mediated nuclear translocation of NF-κB (12). TSG6 also has been shown to reduce inflammation by inhibiting NF-κB signaling in a model of sterile injury of the cornea (11, 31).

Although the anti-inflammatory effects of TSG6 have been well described (1, 2, 7–14, 29, 32), how it modulates inflammation has not been addressed until now. Here, in studies performed in a model of LPS-induced inflammatory lung injury that simulates ALI, we have demonstrated that (*i*) *TSG6*$^{-/-}$ mice exhibit markedly augmented lung vascular injury and neutrophil sequestration and mortality, which is reversed by i.t. TSG6 instillation; (*ii*) i.t. TSG6 instillation even at 6 h after the onset of lung injury reduces mortality by 50% from the 100% mortality seen in untreated control mice; and (*iii*) TSG6 functions by interfering with TLR4–MyD88 interaction in macrophages to inhibit NF-κB and STAT1 and STAT3 activation, and thereby promote the transition of

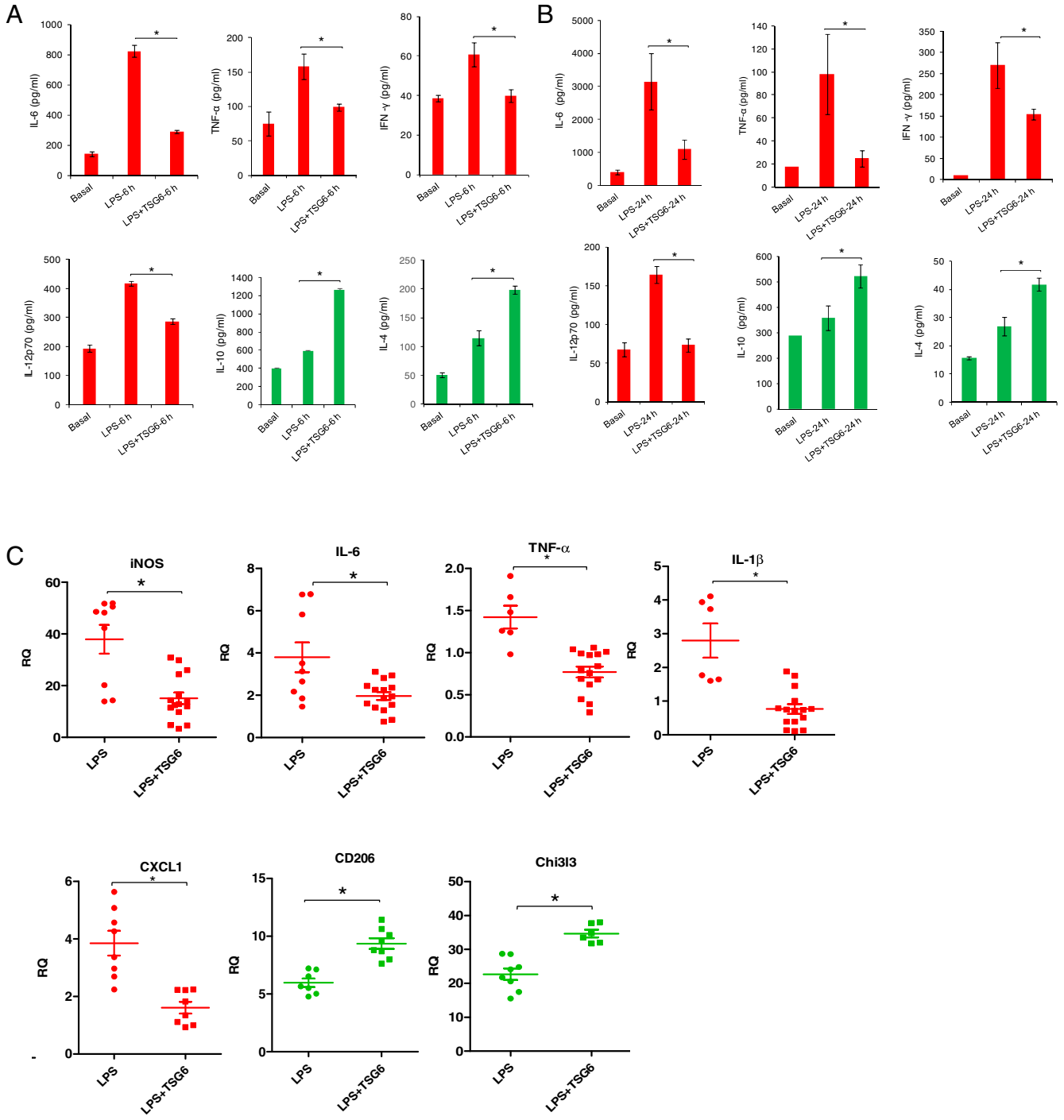

Fig. 3. TSG6 induces expression of anti-inflammatory factors while suppressing proinflammatory factors in alveolar macrophages. (*A* and *B*) Concentrations of proinflammatory cytokines (IL-6, TNFα, IFNγ, and IL12p70) and anti-inflammatory cytokines (IL-10 and IL-4) were measured in BAL fluid of mice challenged with either i.p. LPS (10 mg/kg) and i.t. saline or i.p. LPS (10 mg/kg) and i.t. TSG6 (5 μg) for 6 h (*A*) or 24 h (*B*). TSG6 significantly decreased the production of IL-6, TNFα, IFNγ, and IL-12p70 while increasing the production of IL-10 and IL-4. $n = 4$ mice per group. $^*P < 0.05$. (*C*) Quantification of transcript expression of iNOS, IL-6, IL-1β, TNFα, CXCL1, Chi3l3, and CD206 by qPCR in $CD11b^+$ alveolar macrophages from BAL fluid of mice challenged with either i.p. LPS (10 mg/kg) for 24 h or i.p. LPS (10 mg/kg) and i.t. TSG6 (5 μg) for 24 h. $^*P < 0.05$, LPS vs. LPS + TSG6.

anti- inflammatory macrophages. We also observed that LPS itself up-regulated the expression of TSG6 in lung as reported previously (3–5, 29), consistent with its role as an autocrine mediator resolving inflammatory injury.

NF-κB activation is a known driver of inflammatory signaling (33). Our results show that the rTSG6-mediated suppression of MyD88-dependent NF-κB activation is essential for reprogramming macrophages. Of note, the LPS-induced IKKβ phosphorylation was observed in 5 min, but a strong association of TLR4 and MyD88 was not seen until 15 min. Although the reason for this discrepancy is not clear, the early IKKβ phosphorylation could have been mediated by MyD88-independent pathways (26). In response to

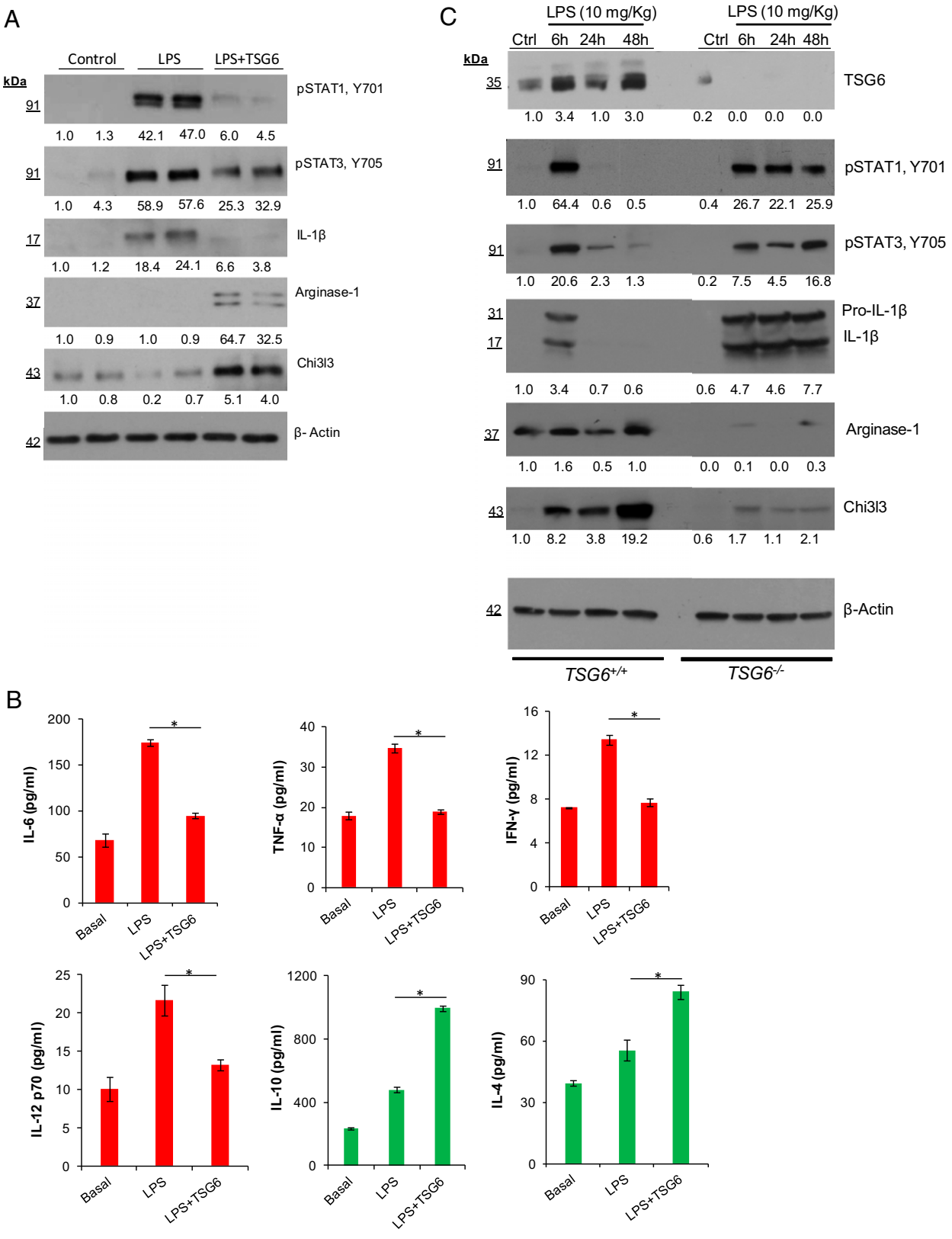

Fig. 4. TSG6 induces suppression of proinflammatory proteins and up-regulation of anti- inflammatory proteins in CD11b$^+$ lung macrophages. (*A*) Immunoblots showing expression of proinflammatory proteins (STAT1, STAT3, and IL-1β) and anti-inflammatory proteins (arginase-1 and Chi3l3) in purified CD11b$^+$ macrophages obtained from lungs of mice challenged with LPS for 24 h. Results are representative of two separate experiments. (*B*) Concentrations of proinflammatory cytokines (IL-6, TNFα, IFNγ, and IL-12p70) and anti-inflammatory cytokines (IL-10 and IL-4) in cultured supernatants of CD11b$^+$ lung macrophages. *$P < 0.05$, LPS vs. LPS + TSG6. (*C*) Immunoblots showing expression of TSG6 and proinflammatory and anti-inflammatory proteins (pSTAT1, pSTAT3, IL-1β, Chi3l3, and arginase-1) in lung lysates of LPS-challenged WT and *TSG6*$^{-/-}$ mice. Results are representative of two separate experiments.

rTSG6, the macrophages shifted from generating proinflammatory cytokines TNFα, IL-1β, IL-6, and IL-12p70 to generating a distinct anti-inflammatory phenotype. NF-κB is normally maintained in an inactive state in the cytoplasm by inhibitory proteins, such as IκB (33). Macrophage polarization to the anti-inflammatory phenotype requires the formation of inactive dimers of the p50 subunit of NF-κB, resulting in suppression of NF-κB–driven macrophage polarization (22). We observed that rTSG6 prevents the interaction of TLR4 with MyD88, a requirement for the activation of NF-κB signaling (33), and that this in turn induces the shift toward anti-inflammatory macrophages. Similar results were seen in a model of zymosan-induced peritonitis in which TSG6 prevented the interaction of TLR2 with MyD88 and thus inhibited the activation of NF-κB (12).

Macrophage polarization is a central feature of inflammatory disease progression, such as in ALI (17, 18). In lungs, resident alveolar macrophages are the first line of defense against airway pathogens. They orchestrate the inflammatory response through activation of pattern recognition receptors that initiate both inflammatory and resolution pathways (17, 18). The phenotype of anti-inflammatory macrophages is characterized by the proteins arginase-1, Chi3l3, pSTAT6, IL-4, and IL-10, whereas proinflammatory macrophages express iNOS, pSTAT1, pSTAT3, TNFα, IL-6, IFNγ, IL-12p70, and IL-1β (17–21, 23, 24). We have shown that TSG6 reprograms macrophages to the anti-inflammatory phenotype, which resolves ALI.

Mice genetically deficient in TSG6 ($TSG6^{-/-}$) exhibited far greater mortality than controls owing to the inability to reprogram macrophages, and thus to resolve ALI. Because TSG6 is released in the inflammatory milieu (3, 29), our finding that TSG6 induces the phenotype switch in macrophages suggests the therapeutic potential of TSG6 in sepsis-induced ALI. Of special note is that the effective dose of TSG6 administered i.t. was only 5 μg, or one-tenth the dose required for efficacy with i.v. administration in several mouse models of inflammation (8–13, 32).

Materials and Methods

Mouse Experiments. All mice were housed at the University of Illinois Animal Care Facility in accordance with institutional guidelines and guidelines of the National Institutes of Health. Veterinary care of the mice and the related animal experiments was approved by the University of Illinois Animal Resources Center. The TSG6 knockout mice originally generated on a BALB/c background (30) were obtained from Jackson Laboratory. Age-matched $TSG6^{+/+}$ and $TSG6^{-/-}$ littermates were used for all experiments.

Endotoxin-Induced ALI and i.t. rTSG6 Instillation. Age- and weight-matched $TSG6^{+/+}$ and $TSG6^{-/-}$ mice received a single i.p. dose of LPS (10 mg/kg body weight; *Escherichia coli* strain 0111:B4; Sigma-Aldrich). The mice were given a single 5-μg dose of rTSG6 (2104-TS-050; R&D Systems) by noninvasive i.t. instillation. For i.t. instillation, the mice were anesthetized by ketamine/xylazine (45 mg/kg and 8 mg/kg, respectively) and were suspended on a flat board and placed in a semirecumbent position with the ventral surface and rostrum facing up. Using a curved blade forceps, the tongue was gently and partially retracted rostrally, and 50 μL containing 5 μg of rTSG6 was placed in the trachea. Saline (50 μL) alone was similarly administered to the control mice. For survival studies, mice injected i.p. with 20 mg/kg LPS were monitored four times daily for up to 3 d.

MPO Assay. MPO activity in lung tissue was measured as described previously (34). The lungs were homogenized in 1 mL of PBS with 0.5% hexadecyltrimethylammonium bromide. The homogenates were sonicated, centrifuged at 40,000 × *g* for 20 min, and run through two freeze-thaw cycles. The samples were homogenized and centrifuged a second time. The supernatant was then collected and mixed 1/30 (vol/vol) with assay buffer (0.2 mg/mL *o*-dianisidine hydrochloride and 0.0005% H_2O_2). The change in absorbance was measured at 460 nm for 3 min, and MPO activity was calculated as the change in absorbance over time.

Measurement of Lung Vascular Permeability. Lung vascular leak was measured using EBA as described previously (35). Mice anesthetized with 2.5% (vol/vol) isoflurane in room air were injected retro-orbitally with 150 μL of EBA (30 mg/kg). At 30 min after EBA injection, animals were killed, and lung tissue was harvested for EBA measurement.

Bone Marrow-Derived Macrophage Cultures. For the isolation of bone marrow cells, femur cavities from WT mice (C57bl/6) were flushed, the cells were plated at approximately 2×10^6 cells/mL, and incubated in DMEM supplemented with 10% (vol/vol) FBS, 1% (vol/vol) streptomycin/penicillin, and 10% (vol/vol) L929-conditioned media for 1 wk. Cells were used for experiments at day 7 of culture.

Immunoprecipitation. Bone marrow-derived macrophages were stimulated with LPS (1 μg/mL) alone or in combination with TSG6 (0.1 μg/mL) for 0, 5, 15, and 30 min. After this treatment, cells were lysed in lysis buffer (final concentration: 10 mM Tris·HCl, 150 mM NaCl, 1 mM EDTA, 1 mM EGTA, 1 mM PMSF, 1 mM sodium vanadate, 1% Triton X100, and 0.5% Nonidet P-40) supplemented with protease inhibitor mixture. The cell lysate was cleared of cellular debris by centrifuging at 12,000 × *g* for 10 min. The clear supernatant collected was subjected to immunoprecipitation. Each sample was incubated overnight with TLR4 antibody (1 μg/mL) at 4 °C on a rotating platform. Next day, protein A/G beads were added to the sample and incubated for 1 h at 4 °C. Immunoprecipitated samples were washed three times and used for immunoblotting.

Immunostaining. Bone marrow-derived macrophages from mice grown on coverslips were stimulated with LPS (1 μg/mL) alone or in combination with TSG6 (0.1 μg/mL) for 0 and 15 min. After this treatment, cells were fixed and used for immunostaining (36).

Collection of BAL Fluid and Cells. For collection of BAL fluid, the upper part of the trachea was cannulated and then lavaged three times with 0.8 mL of PBS supplemented with 0.4 mM EDTA and protease inhibitor mixture. The fluid recovery rate typically exceeds 90%. The lavage samples from each mouse were kept on ice. BAL fluid was centrifuged at 700 × *g* for 5 min at 4 °C. The collected supernatant was then used for cytokine assays.

Immunoblotting. Cells were lysed in lysis buffer (50 mM Tris·HCl pH 7.5, 150 mM NaCl, 1 mM EGTA, 1% Triton X-100, 0.25% sodium deoxycholate, 0.1% SDS, and protease inhibitor mixture). Mouse lungs were homogenized in lysis buffer (35). Cell lysates or mouse lung homogenates were centrifuged at 14,000 × *g* at 4 °C for 10 min, and cleared supernatant was used for immunoblot analysis. The protein lysates were resolved by SDS/PAGE on a 4–15% gradient separating gel under reducing conditions and transferred to PVDF membrane. The membrane was blocked with 3% (wt/vol) BSA in TBST (10 mM Tris·HCl pH 7.5, 150 nM NaCl, and 0.05% Tween-20) for 1 h at room temperature. The membranes were then probed with the indicated primary antibody (diluted in blocking buffer) overnight at 4 °C. Next, membranes were washed three times and then incubated with an appropriate HRP-conjugated secondary antibody. Protein bands were detected by enhanced chemiluminescence. The following antibodies were used for immunoblotting: TSG6 (MAB-2104; R&D Systems), TLR4 (sc-30002; Santa Cruz Biotechnology), MyD88 (sc-8196; Santa Cruz Biotechnology), phospho-$STAT1^{Y701}$ (612233; BD Biosciences), phospho-$STAT3^{Y705}$ (51-9002097; BD Biosciences), Chi3l3 (AF2446; R&D Systems), Arginase-1 (610708; BD Biosciences), IL-1β (AF401; R&D Systems), phospho-IKKα/β (2697; Cell Signaling Technology), total IKK (2684; Cell Signaling Technology), and anti–β-actin (A5316, mouse monoclonal; Sigma-Aldrich). Band intensity was determined by densitometry with the aid of ImageJ software.

Cytokine ELISA. Cytokines were measured in BAL fluid and supernatants of cultured macrophages with commercially available ELISA kits (eBioscience) according to the manufacturer's instructions.

Isolation of $CD11b^+$ Alveolar Macrophages. The $CD11b^+$ cells were isolated from total BAL fluid by incubation with $CD11b^+$ magnetic beads (Miltenyi Biotec) (37) according to the manufacturer's instructions. For isolation of $CD11b^+$ cells from the lungs, the harvested lungs were minced into small pieces and then incubated in DMEM with 1% penicillin-streptomycin for 30 min at 37 °C and 5% (vol/vol) CO_2 in the presence of 1 mg/mL collagenase A (70499828; Roche). After incubation, the minced pieces of lungs were passed through 16G and 18G needles, and the resulting suspension was passed through a 70-μm cell strainer and then washed with complete DMEM. The cells were centrifuged at 200 × *g* for 3 min, incubated for 20 min at 4 °C with CD11b magnetic beads, and finally applied and eluted from MS columns (Miltenyi Biotec) for the positive selection of $CD11b^+$ cells.

RNA Extraction and qRT-PCR. Total RNA isolated from CD11b$^+$ cells was reverse-transcribed with random hexamers and MultiScribe reverse transcriptase (Applied Biosystems). The cDNA thus obtained was mixed with SYBR Green PCR Master Mix (Applied Biosystems) and gene-specific primers for PCR. An ABI Prism 7000 was used for quantitative PCR analysis. Cyclophilin expression served as an internal control. The following mouse primers were used: iNOS (forward, 5′-AGTCTCAGACATGGCTTGCCCCT-3′; reverse, 5′-GCTGCGGGGAGCCATTTTGGT-3′), IL-6 (forward, 5′-TCCAGTTGCCTTCTTGGGACTG-3′; reverse, 5′-AGCCTCCGACTTGTGAAGTGGT-3′), TNFα (forward, 5′-GACCCTCACACTCAGATCATCT-3′; reverse, 5′-CCTCCACTTGGTGGTTTGCT-3′), IL-1β (forward, 5′-GAATCTATACCTGTCCTGTG-3′; reverse, 5′-TTATGTCCTGACCACTGTTG-3′), CXCL1 (forward, 5′- CTGGGATTCACCTCAAGAACATC-3′; reverse, 5′-CAGGGTCAAGGCAAGCCTC-3′), Chi3l3 (forward, 5′-AGAAGGGAGTTTCAAACCTGGT-3′; reverse, 5′-GTCTTGCTCATGTGTGTAAGTGA-3′), CD206 (forward, 5′-CCACGGATGACCTGTGCTCGAG-3′; reverse, 5′- ACACCAGAGCCATCCGTCCGA-3′), and CYP (forward, 5′-CTTGTCCATGGCAAATGCTG-3′; reverse, 5′-GTGATCTTCTTGCTGGTCTTGC-3′).

Statistical Analysis. Data were analyzed using the unpaired Student's *t* test and log-rank test. A difference in mean values was considered significant at a P value <0.05.

ACKNOWLEDGMENTS. This work was supported in part by American Heart Association Scientist Development Grant 16SDG30980061 (to M.M.) and National Institutes of Health Grants P01 HL077806, R01 HL122157, R01 HL125350, P40OD011050, and R01 HL128359.

1. Prockop DJ (2016) Inflammation, fibrosis, and modulation of the process by mesenchymal stem/stromal cells. *Matrix Biol* 51:7–13.
2. Lee RH, et al. (2014) TSG-6 as a biomarker to predict efficacy of human mesenchymal stem/progenitor cells (hMSCs) in modulating sterile inflammation in vivo. *Proc Natl Acad Sci USA* 111(47):16766–16771.
3. Milner CM, Day AJ (2003) TSG-6: A multifunctional protein associated with inflammation. *J Cell Sci* 116(Pt 10):1863–1873.
4. Wisniewski HG, Vilcek J (2004) Cytokine-induced gene expression at the crossroads of innate immunity, inflammation and fertility: TSG-6 and PTX3/TSG-14. *Cytokine Growth Factor Rev* 15(2-3):129–146.
5. Wisniewski HG, et al. (1993) TSG-6: a TNF-, IL-1-, and LPS-inducible secreted glycoprotein associated with arthritis. *J Immunol* 151(11):6593–6601.
6. Lesley J, et al. (2004) TSG-6 modulates the interaction between hyaluronan and cell surface CD44. *J Biol Chem* 279(24):25745–25754.
7. Dyer DP, et al. (2016) The anti-inflammatory protein TSG-6 regulates chemokine function by inhibiting chemokine/glycosaminoglycan interactions. *J Biol Chem* 291(24):12627–12640.
8. Getting SJ, et al. (2002) The link module from human TSG-6 inhibits neutrophil migration in a hyaluronan- and inter-alpha inhibitor-independent manner. *J Biol Chem* 277(52):51068–51076.
9. Mindrescu C, et al. (2002) Reduced susceptibility to collagen-induced arthritis in DBA/1J mice expressing the TSG-6 transgene. *Arthritis Rheum* 46(9):2453–2464.
10. Lee RH, et al. (2009) Intravenous hMSCs improve myocardial infarction in mice because cells embolized in lung are activated to secrete the anti-inflammatory protein TSG-6. *Cell Stem Cell* 5(1):54–63.
11. Oh JY, et al. (2010) Anti-inflammatory protein TSG-6 reduces inflammatory damage to the cornea following chemical and mechanical injury. *Proc Natl Acad Sci USA* 107(39):16875–16880.
12. Choi H, Lee RH, Bazhanov N, Oh JY, Prockop DJ (2011) Anti-inflammatory protein TSG-6 secreted by activated MSCs attenuates zymosan-induced mouse peritonitis by decreasing TLR2/NF-κB signaling in resident macrophages. *Blood* 118(2):330–338.
13. Danchuk S, et al. (2011) Human multipotent stromal cells attenuate lipopolysaccharide-induced acute lung injury in mice via secretion of tumor necrosis factor-α induced protein 6. *Stem Cell Res Ther* 2(3):27.
14. Kota DJ, Wiggins LL, Yoon N, Lee RH (2013) TSG-6 produced by hMSCs delays the onset of autoimmune diabetes by suppressing Th1 development and enhancing tolerogenicity. *Diabetes* 62(6):2048–2058.
15. Bhattacharya J, Matthay MA (2013) Regulation and repair of the alveolar-capillary barrier in acute lung injury. *Annu Rev Physiol* 75:593–615.
16. Kawai T, Akira S (2011) Toll-like receptors and their crosstalk with other innate receptors in infection and immunity. *Immunity* 34(5):637–650.
17. Hussell T, Bell TJ (2014) Alveolar macrophages: Plasticity in a tissue-specific context. *Nat Rev Immunol* 14(2):81–93.
18. Kopf M, Schneider C, Nobs SP (2015) The development and function of lung-resident macrophages and dendritic cells. *Nat Immunol* 16(1):36–44.
19. Mosser DM, Edwards JP (2008) Exploring the full spectrum of macrophage activation. *Nat Rev Immunol* 8(12):958–969.
20. Murray PJ, et al. (2014) Macrophage activation and polarization: Nomenclature and experimental guidelines. *Immunity* 41(1):14–20.
21. Lawrence T, Natoli G (2011) Transcriptional regulation of macrophage polarization: Enabling diversity with identity. *Nat Rev Immunol* 11(11):750–761.
22. Porta C, et al. (2009) Tolerance and M2 (alternative) macrophage polarization are related processes orchestrated by p50 nuclear factor kappaB. *Proc Natl Acad Sci USA* 106(35):14978–14983.
23. Sica A, Mantovani A (2012) Macrophage plasticity and polarization: In vivo veritas. *J Clin Invest* 122(3):787–795.
24. Mantovani A, Biswas SK, Galdiero MR, Sica A, Locati M (2013) Macrophage plasticity and polarization in tissue repair and remodeling. *J Pathol* 229(2):176–185.
25. Takaoka Y, et al. (2014) Glyceraldehyde-3-phosphate dehydrogenase (GAPDH) prevents lipopolysaccharide (LPS)-induced, sepsis-related severe acute lung injury in mice. *Sci Rep* 4:5204.
26. Andreakos E, et al. (2004) Distinct pathways of LPS-induced NF-kappa B activation and cytokine production in human myeloid and nonmyeloid cells defined by selective utilization of MyD88 and Mal/TIRAP. *Blood* 103(6):2229–2237.
27. Lee TH, Lee GW, Ziff EB, Vilcek J (1990) Isolation and characterization of eight tumor necrosis factor-induced gene sequences from human fibroblasts. *Mol Cell Biol* 10(5):1982–1988.
28. Lee TH, Wisniewski HG, Vilcek J (1992) A novel secretory tumor necrosis factor-inducible protein (TSG-6) is a member of the family of hyaluronate binding proteins, closely related to the adhesion receptor CD44. *J Cell Biol* 116(2):545–557.
29. Prockop DJ, Oh JY (2012) Mesenchymal stem/stromal cells (MSCs): Role as guardians of inflammation. *Mol Ther* 20(1):14–20.
30. Szántó S, Bárdos T, Gál I, Glant TT, Mikecz K (2004) Enhanced neutrophil extravasation and rapid progression of proteoglycan-induced arthritis in TSG-6-knockout mice. *Arthritis Rheum* 50(9):3012–3022.
31. Oh JY, et al. (2012) Identification of the HSPB4/TLR2/NF-κB axis in macrophage as a therapeutic target for sterile inflammation of the cornea. *EMBO Mol Med* 4(5):435–448.
32. Foskett AM, et al. (2014) Phase-directed therapy: TSG-6 targeted to early inflammation improves bleomycin-injured lungs. *Am J Physiol Lung Cell Mol Physiol* 306(2):L120–L131.
33. Li Q, Verma IM (2002) NF-kappaB regulation in the immune system. *Nat Rev Immunol* 2(10):725–734.
34. Hickey MJ, et al. (2002) Inducible nitric oxide synthase (iNOS) in endotoxemia: chimeric mice reveal different cellular sources in various tissues. *FASEB J* 16(9):1141–1143.
35. DebRoy A, et al. (2014) Cooperative signaling via transcription factors NF-κB and AP1/c-Fos mediates endothelial cell STIM1 expression and hyperpermeability in response to endotoxin. *J Biol Chem* 289(35):24188–24201.
36. Mittal M, et al. (2015) Novel role of reactive oxygen species-activated Trp melastatin channel-2 in mediating angiogenesis and postischemic neovascularization. *Arterioscler Thromb Vasc Biol* 35(4):877–887.
37. Németh K, et al. (2009) Bone marrow stromal cells attenuate sepsis via prostaglandin E(2)-dependent reprogramming of host macrophages to increase their interleukin-10 production. *Nat Med* 15(1):42–49.